

Evaluation of Sea Surface Temperature From FY-3C VIRR Data in the Arctic

Hongyan Wang, Lei Guan, *Member, IEEE*, and Ge Chen

Abstract—Daily 5-km sea surface temperature (SST) data from the Visible and Infrared Scanning Radiometer (VIRR) onboard the Fengyun-3C (FY-3C) satellite are evaluated for latitudes greater than 60° N against *in situ* and daily 4-km SST data from the Moderate Resolution Imaging Spectroradiometer (MODIS) onboard the Terra satellite. Approximately five months of data are used for the evaluation, during August to December 2014. The *in situ* and 4-km MODIS SST data are averaged and resampled at a spatial resolution of 5 km, which is similar to that of the VIRR SST data. The bias and standard deviation of the SST difference between VIRR and buoy data are -0.12°C and 0.93°C , respectively. A three-way error analysis is conducted between VIRR, MODIS, and buoy SSTs to obtain standard deviations of error for each kind of observation. The separated standard deviations of the error are found to be 0.91°C for the VIRR SST, 0.20°C for the *in situ* SST, and 0.51°C for the MODIS SST. The error sources are discussed. The results indicate that the FY-3C/VIRR SST product needs to be improved.

Index Terms—Arctic, Fengyun-3C (FY-3C), Moderate Resolution Imaging Spectroradiometer (MODIS), Sea Surface Temperature (SST), Visible and Infrared Scanning Radiometer (VIRR).

I. INTRODUCTION

SEA surface temperatures (SSTs) derived from satellite observations are important oceanographic and air-sea flux indicators. SST is a key parameter in ocean and atmospheric models because it represents the lower boundary of the atmosphere and oceans [1]–[5], and a long-term series of SST data can be used to monitor and predict climate change [6]–[8]. Accuracies of 0.5 K, 0.2 K, and 0.1 K are desired for coastal or local applications, ocean forecasting, and climate monitoring at spatial resolutions of ≤ 0.5 , 1–10, and 10–50 km, respectively [9]. Satellite SST observations have the advantage of spatial coverage, and infrared instruments onboard polar-orbiting or geostationary satellites are able to measure SST at a spatial resolution of 1–4 km. However, Arctic cloud coverage values of up to 90% during the summer and 50%–60% during the winter have been reported based on surface and satellite observations

Manuscript received August 25, 2015; revised November 29, 2015; accepted December 18, 2015. Date of publication January 8, 2016; date of current version January 19, 2016. This work was supported by the Global Change Research Program of China under Grant 2015CB953901, National Natural Science Foundation of China (NSFC)-Shandong Joint Fund for Marine Science Research Centers under Grant U1406404, NSFC project 41376105, and SRFDP project 20130132110013.

The authors are with the Department of Marine Technology, College of Information Science and Engineering, Ocean University of China, Qingdao 266100, China (e-mail: wanghongyan2011@gmail.com).

Color versions of one or more of the figures in this paper are available online at <http://ieeexplore.ieee.org>.

Digital Object Identifier 10.1109/LGRS.2015.2511184

[10]. Thus, persistent Arctic cloud coverage occurs throughout the year [11], [12]. Extreme atmospheric conditions, sparse *in situ* measurements, and persistent cloud cover pose challenges to retrieving and evaluating Arctic SST from satellite data [13]–[15]. The daily Moderate Resolution Imaging Spectroradiometer onboard Terra (Terra/MODIS) Level-3 SST products with the highest quality flag have been found to have a bias of -0.46 K and standard deviation (Std) of 0.66 K during the nighttime based on comparisons with buoy data [14].

The objective of this study is to evaluate the SST products from the Fengyun-3C Visible and Infrared Scanning Radiometer (FY-3C/VIRR) in the Arctic versus *in situ* measurements and Terra/MODIS SST products.

Satellite and *in situ* data are described in Section II of this letter. The corresponding matchup procedures and evaluation results are given in Section III, followed by the conclusion in Section IV.

II. DATA

A. FY-3C/VIRR SST

FY-3 series satellites are the second-generation polar-orbiting meteorological satellites from China. Three satellites have been launched. FY-3A and FY-3B were launched as experimental satellites on May 27, 2008, and November 5, 2010, respectively. FY-3C was launched as an operational satellite on September 23, 2013. FY-3C has an equator crossing time of 10:00 A.M. in the descending node and a designed life span of five years. The VIRR instrument onboard FY-3C has 10 spectral bands, ranging from 0.43 to $12.5\text{ }\mu\text{m}$, with a resolution of 1.1 km at nadir and swath of 2800 km [16]. The VIRR has infrared split-window channels (10.3 – 11.3 and 11.5 – $12.5\text{ }\mu\text{m}$) for SST observations. Spectral features provide a noise equivalent temperature at infrared channels of 0.2 K [16].

The 5-km daily-composited daytime and nighttime FY-3C VIRR SST products are distributed by the National Satellite Meteorological Center (NSMC) and China Meteorological Administration (CMA). They have been available from May 4, 2014, to the present (<http://fy3.satellite.cma.gov.cn/PortalSite/Data/Satellite.aspx>). The operational FY-3C/VIRR SST algorithm is a multichannel SST algorithm [16], [17]. Due to sparse data availability from May to July, only the data from August to December 2014 are used in this study.

The VIRR SST products are distributed as bulk SST data because *in situ* observations are used to tune the algorithm coefficients [16]. Wang *et al.* [16] reported biases of -0.26 K and 0.06 K and standard deviations of 0.54 K and 0.56 K for daytime and nighttime data as compared to monthly global

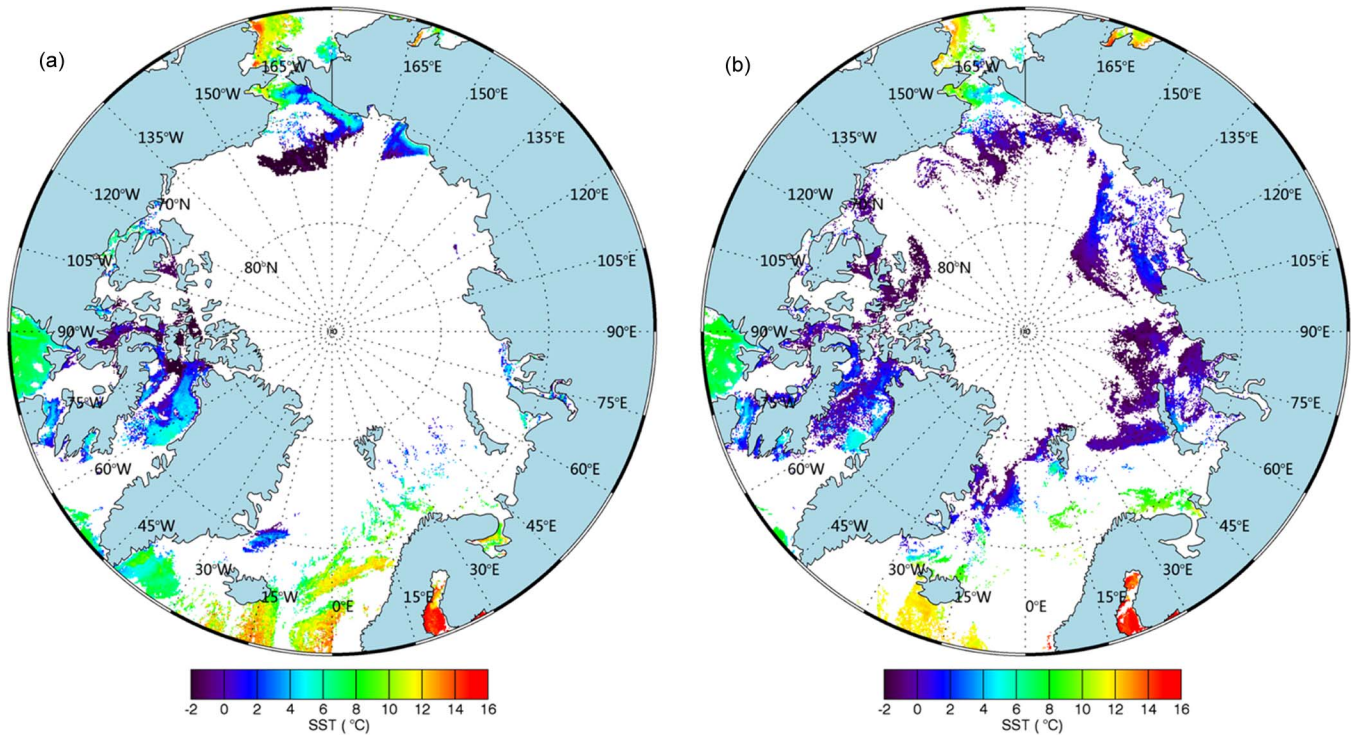


Fig. 1. Example of Arctic SSTs (night, September 5, 2014). (a) VIRR SST. (b) MODIS SST.

VIRR SST and *in situ* data, respectively. An example of VIRR SST in the Arctic is shown in Fig. 1(a). White color indicates cloudy pixels or invalid data.

B. Terra/MODIS SST

The MODIS instrument is onboard the Terra satellite, which was launched on December 18, 1999. Terra has an equator crossing time of 10:30 A.M. in the descending node and a designed life span of six years. The MODIS instrument has 36 spectral bands, ranging from 0.4 to 14.4 μm , with a swath of 2330 km (cross track) and a resolution of 1 km at nadir.

The daily-composited 4-km MODIS Level-3 Standard Mapped Image SST products used in this study are obtained from the NASA OceanColor website (<http://oceancolor.gsfc.nasa.gov/>), which provides daytime and nighttime products.

The MODIS long-wave (11–12 μm) SST algorithm is a nonlinear SST algorithm [18]. MODIS SST data have been adjusted to skin SST [19]–[21]. The SST products possess quality flags of 0–2, where 0 represents the highest quality and 2 is the lowest quality. Only the highest quality SST data are used in this study. An example of MODIS SSTs in the Arctic is shown in Fig. 1(b). The cloud detection and sea ice flag algorithms as well as other quality flag procedures are possible reasons for the different coverage, as shown in Fig. 1(a) and (b).

C. In Situ Data

The *in situ* SST quality monitor (iQuam) system was developed by the Center for Satellite Applications and Research (STAR), National Oceanic and Atmospheric Administration (NOAA) Satellite and Information Service (NESDIS), to per-

form near-real-time quality control of *in situ* measurements, monitor statistics, and assign quality flags to reformat Global Telecommunication System (GTS) SST data [22]. Data from ships and buoys (drifters and moorings) are included in the system. Monthly data are available from NCEP GTS every 12 h, and *in situ* data are available via FTP (<http://www.star.nesdis.noaa.gov/sod/sst/iquam/index.html>). Only drifting and mooring buoy SST data are used in this study to evaluate the VIRR SST because they possess a higher quality than other types of *in situ* data [14], [23]–[26].

III. EVALUATION OF VIRR SST DATA USING MODIS AND BUOY SSTs

A. Matchup Data Sets

The study area focuses on latitudes greater than 60° N using data from August to December 2014. First, matchup data sets within collocated spatial and temporal windows are generated using VIRR, MODIS, and buoy data. The spatial window is 5 km, which represents one VIRR SST grid size. Studies have shown that a significant diurnal warming event, with a diurnal warming amplitude of 1.5 K for moored buoy at a depth of 0.5 m, is found at high latitudes during the summer months [27]. Thus, only nighttime SST products and buoy data are used to minimize the diurnal warming effect in this study. Nighttime buoy SSTs with solar zenith angles larger than 85°, which is the same threshold as the MODIS day and night flag [28], are selected using solar zenith angles calculated based on observation date, time, and location information. The nighttime buoy and MODIS SSTs are then averaged to obtain daily SSTs at a resolution of 5 km. The initial matchup data set, which

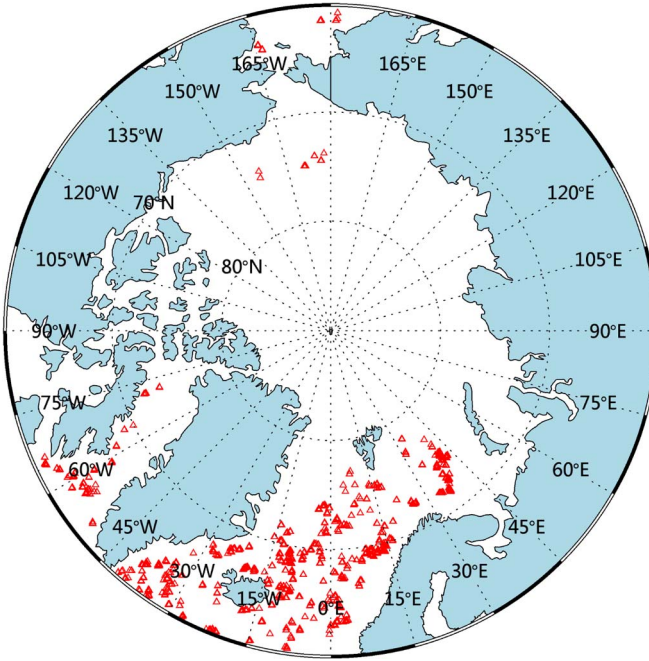


Fig. 2. Locations of matchups between satellite sensors, VIRR, MODIS, and buoy data.

includes a total number of 2472, is generated between the VIRR, MODIS, and buoy SSTs for the Arctic.

The disparity between the satellite and buoy SST spatial resolutions may cause large errors in areas with strong SST gradients. The buoy SST variation within a 5-km grid is investigated. A maximum of 17 buoy data observations are obtained for each 5-km grid during the study period, and approximately 50% of the matchups contain at least three buoy observations in each grid. Furthermore, various block size tests (3×3 , 5×5 , 7×7 , and 9×9) are conducted based on the initial matchups to identify cloudy pixels and minimize the influence of thin clouds. A pixel is identified clear only if all of the pixels in the block size are clearly observations. Thus, new matchup data sets are generated after the block tests. The total number in the matchup data set decreases as the block size increases. The number of matchups is 1032 after the 9×9 block test, minimizing the thin-cloud effect. The location of the matchups after removing the outliers is shown in Fig. 2, in which red triangles indicate locations where VIRR, MODIS, and buoy SSTs are compared. The matchups are mainly located in the Nordic Seas, Denmark Strait, Davis Strait, Baffin Bay, Bering Sea, and Beaufort Sea (Fig. 2).

B. Evaluation of VIRR and MODIS Data With Buoy SSTs

Evaluations are conducted between VIRR and buoy SSTs, and MODIS and buoy SSTs using the matchup data set generated in section three. The 9×9 block test yields the best performance. The data are described based on the bias, standard deviation, median, and robust standard deviation (RSD) [29]–[31]. The outliers are removed using three times the RSD from the median in this study [30]–[34]. The bias and standard deviation (VIRR minus buoy) are -0.47°C and 1.48°C for the

TABLE I
STATISTICS BETWEEN VIRR, BUOY, AND MODIS SSTs FROM 2014

	N	Bias($^{\circ}\text{C}$)	Std($^{\circ}\text{C}$)	Median($^{\circ}\text{C}$)	RSD($^{\circ}\text{C}$)	P($\pm 0.5^{\circ}\text{C}$) (%)
VIRR – buoy	1032	-0.12	0.93	-0.06	0.76	49
MODIS-buoy	1032	-0.61	0.55	-0.56	0.48	45
VIRR-MODIS	1032	0.49	1.04	0.49	1.01	36

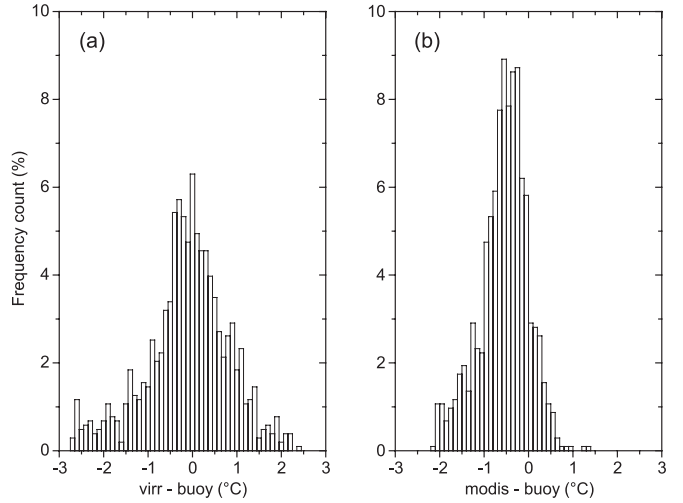


Fig. 3. Histograms of the SST differences between the satellite and buoy data. (a) VIRR minus buoy. (b) MODIS minus buoy.

initial VIRR and buoy matchups, respectively. The results shown in Table I display a bias of -0.12°C and a standard deviation of 0.93°C for 1032 VIRR and buoy matchups (VIRR minus buoy). The bias and standard deviation are about 0.4°C and 0.5°C smaller after the block test. The results before and after the block tests clearly indicate that cloud contamination and the SST algorithm influence the VIRR SST. The VIRR and buoy SST data distribution histograms are shown in Fig. 3(a). The VIRR and buoy statistics indicate a median of -0.06°C and an RSD of 0.76°C , with a $P(\pm 0.5^{\circ}\text{C})$ of 49%, where $P(\pm 0.5^{\circ}\text{C})$ is the proportion of the SST difference within $\pm 0.5^{\circ}\text{C}$.

A 0.17 K offset is added to the Terra/MODIS nighttime SSTs to adjust the MODIS skin to the bulk temperature, allowing for a comparison with buoy SSTs [13], [14], [35]. The results indicate a bias (MODIS minus buoy) of -0.68°C and a standard deviation of 0.59°C before the block tests and a bias of -0.61°C and a standard deviation of 0.55°C after the block tests (Table I). The MODIS SST cloud detection algorithm consists of a series threshold, spatial homogeneity tests, and a delta climatology test [20]. The results reveal that the MODIS SST algorithm is robust, and the complicated MODIS SST cloud detection algorithm performs well. The MODIS and buoy data distribution histograms are shown in Fig. 3(b). The MODIS and buoy statistics indicate a median of -0.56°C and an RSD of 0.48°C , with a $P(\pm 0.5^{\circ}\text{C})$ of 45%.

The time series of matchups for SST difference between the satellite and buoy SSTs are shown in Fig. 4. The SST difference between the VIRR and buoy SSTs encompasses a warm bias after October, whereas a cool bias exists for the SST difference between the MODIS and buoy SSTs. The cool bias trend between the MODIS and buoy data after October is similar to

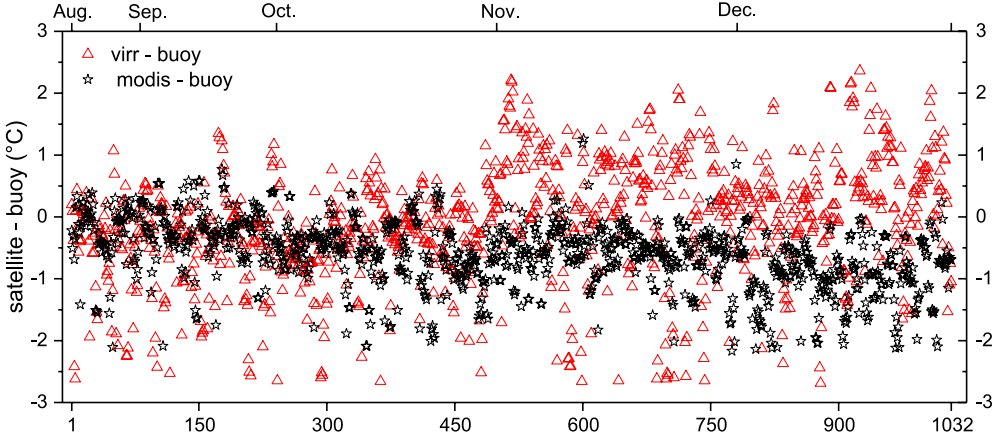


Fig. 4. Time series of matchups between the satellite and buoy SSTs. Red triangle: VIRR minus buoy. Black star: MODIS minus buoy.

that identified by Høyer *et al.* [13]. The SST algorithm may contribute to this bias when the column water vapor decreases during the Arctic winter. In addition, marginal ice zone effects are not ignorable. Høyer *et al.* reported a significantly high error standard deviation for Terra MODIS within 150 km off the ice [13]. The SST difference between the VIRR and MODIS (VIRR minus MODIS) data exhibits a bias of approximately 0.5 °C, a standard deviation of 1.04 °C, as shown in Table I, and a minimum $P(\pm 0.5 \text{ }^{\circ}\text{C})$ of 36%. The difference between the bias, median, standard deviation, and RSD indicates a low effect of outliers for SST difference.

C. Three-Way Error Analysis

A three-way error analysis is performed to estimate the standard deviation of the error for different observation types. O'Carroll *et al.* [36] evaluated SST data using AATSR, AMSR-E, and *in situ* data. In addition, numerous other studies have utilized three-way error analyses, including Stofflen [37] for wind speed evaluation, Xu and Ignatov [38], Merchant *et al.* [34], O'Carroll *et al.* [39], Lean and Saunders [40], and Gentemann [24] for SST evaluations. The error variance expressions for three different observation types are given by O'Carroll *et al.* [36]

$$\begin{aligned} \sigma_1^2 &= \frac{1}{2}(V_{12} + V_{31} - V_{23}) \\ \sigma_2^2 &= \frac{1}{2}(V_{23} + V_{12} - V_{31}) \\ \sigma_3^2 &= \frac{1}{2}(V_{31} + V_{23} - V_{12}) \end{aligned} \quad (1)$$

where 1, 2, and 3 indicate the three different observation types, V_{ij} is the variance of the difference between observation types i and j, and σ_i^2 is the estimated error variance for observation type i. In this letter, subscript 1 refers to VIRR data, 2 corresponds to *in situ* data, and 3 indicates MODIS data.

Using the standard deviations of the matchups presented in Table I, the standard deviation of the error can be calculated for each observation type. The results indicate standard deviations of the error of 0.91 °C for VIRR, 0.20 °C for buoy, and 0.51 °C

TABLE II
DERIVED STANDARD DEVIATIONS FOR DIFFERENT OBSERVATIONS

	Std (°C)
VIRR	0.91
Buoy	0.20
MODIS	0.51

for MODIS SST, respectively (Table II). The buoy observations exhibit the smallest error, whereas the MODIS accuracy is consistent with the findings of Høyer *et al.* [13].

IV. CONCLUSION

The five-month FY-3C VIRR daily nighttime SST products are compared with MODIS and buoy SST data in the Arctic. The results demonstrate that VIRR SSTs exhibit a larger error than buoy SSTs, with a negative bias of $-0.12 \text{ }^{\circ}\text{C}$ and a standard deviation of 0.93 °C. The bias and standard deviation between the MODIS and buoy SST data are $-0.61 \text{ }^{\circ}\text{C}$ and 0.55 °C, displaying a similar accuracy from Høyer *et al.* [13], [14]. The difference between the bias, median, standard deviation, and RSD for VIRR and buoy indicates a high outlier effect. A three-way error analysis indicates standard deviations of the error of 0.91 °C for VIRR, 0.20 °C for buoy, and 0.51 °C for MODIS data, respectively. VIRR SSTs are slightly higher than MODIS SSTs. The various SST algorithms and cloud detection failures could contribute to this error. Studies should focus on robust VIRR SST algorithms and cloud detection algorithms in the future.

ACKNOWLEDGMENT

The authors would like to thank the anonymous reviewers for their helpful suggestions and comments. The FY-3C/VIRR SST products were provided by the NSMC Fengyun Satellite Data Center. Terra/MODIS SST products were provided by the OceanColor Web of NASA. *In situ* SST data were provided by the iQuam system, which was developed by NESDIS/STAR.

REFERENCES

- [1] J. A. Carton, G. Chepurin, X. Cao, and B. Giese, "A simple ocean data assimilation analysis of the global upper ocean 1950–95. Part I: Methodology," *J. Phys. Oceanogr.*, vol. 30, no. 2, pp. 294–309, Feb. 2000.
- [2] J. Larsen, J. L. Høyer, and J. She, "Validation of a hybrid optimal interpolation and Kalman filter scheme for sea surface temperature assimilation," *J. Mar. Syst.*, vol. 65, no. 1–4, pp. 122–133, Mar. 2007.
- [3] N. A. Rayner *et al.*, "Global analyses of sea surface temperature, sea ice, and night marine air temperature since the late nineteenth century," *J. Geophys. Res., Atmos.*, vol. 108, no. D14, p. 4407, Jul. 2003.
- [4] C. A. Clayson and A. S. Bogdanoff, "The effect of diurnal sea surface temperature warming on climatological air-sea fluxes," *J. Clim.*, vol. 26, no. 8, pp. 2546–2556, Nov. 2012.
- [5] X. Song and L. Yu, "High-latitude contribution to global variability of air-sea sensible heat flux," *J. Clim.*, vol. 25, no. 10, pp. 3515–3531, Jan. 2012.
- [6] J. J. Bates and H. F. Diaz, "Evaluation of multichannel sea surface temperature product quality for climate monitoring: 1982–1988," *J. Geophys. Res. Oceans*, vol. 96, no. C11, pp. 20613–20622, Nov. 1991.
- [7] C. K. Folland *et al.*, "Global temperature change and its uncertainties since 1861," *Geophys. Res. Lett.*, vol. 28, no. 13, pp. 2621–2624, Jul. 2001.
- [8] A. Kaplan *et al.*, "Analyses of global sea surface temperature 1856–1991," *J. Geophys. Res., Oceans*, vol. 103, no. C9, pp. 18 567–18 589, Aug. 1998.
- [9] C. J. Donlon, "Sentinel-3 Mission Requirements Traceability Document (MRTD)," European Space Agency, Noordwijk, The Netherlands, no. 1, Feb. 2011.
- [10] J. P. Peixoto and A. H. Oort, *Physics of Climate*. New York, NY, USA: American Institute of Physics, 1992.
- [11] R. Eastman and S. G. Warren, "Arctic cloud changes from surface and satellite observations," *J. Clim.*, vol. 23, no. 15, pp. 4233–4242, Aug. 2010.
- [12] A. J. Schweiger, "Changes in seasonal cloud cover over the Arctic seas from satellite and surface observations," *Geophys. Res. Lett.*, vol. 31, no. 12, Jun. 2004, Art. ID L12207.
- [13] J. L. Høyer, I. Karagali, G. Dybkjær, and R. Tonboe, "Multi sensor validation and error characteristics of Arctic satellite sea surface temperature observations," *Remote Sens. Environ.*, vol. 121, pp. 335–346, Jun. 2012.
- [14] J. L. Høyer, P. Le Borgne, and S. Eastwood, "A bias correction method for Arctic satellite sea surface temperature observations," *Remote Sens. Environ.*, vol. 146, pp. 201–213, Apr. 2014.
- [15] C. Donlon *et al.*, "Successes and challenges for the modern sea surface temperature observing system," in Proc. OceanObs, Sustained Inf. Soc., Venice, Italy, Sep. 21–25, 2009, vol. 2, pp. 1–45.
- [16] S. Wang *et al.*, "FY-3C/VIRR SST algorithm and cal/val activities at NSMC/CMA," in Proc. SPIE, Ocean Remote Sens. Monit. Space, Beijing, China, 2014, vol. 9261, p. 92610G.
- [17] E. P. McClain, W. G. Pichel, C. C. Walton, Z. Ahmad, and J. Sutton, "Multi-channel improvements to satellite-derived global sea surface temperatures," *Adv. Space Res.*, vol. 2, no. 6, pp. 43–47, 1982.
- [18] C. C. Walton, W. G. Pichel, J. F. Sapper, and D. A. May, "The development and operational application of nonlinear algorithms for the measurement of sea surface temperatures with the NOAA polar-orbiting environmental satellites," *J. Geophys. Res., Oceans*, vol. 103, no. C12, pp. 27 999–28 012, Nov. 1998.
- [19] K. A. Kilpatrick *et al.*, "A decade of sea surface temperature from MODIS," *Remote Sens. Environ.*, vol. 165, pp. 27–41, Aug. 2015.
- [20] O. B. Brown and P. J. Minnett, "MODIS Infrared Sea Surface Temperature Algorithm (Algorithm Theoretical Basis Document)," Univ. Miami, Miami, FL, USA, Apr. 1999.
- [21] M. Szczodrak, P. J. Minnett, and R. H. Evans, "The effects of anomalous atmospheres on the accuracy of infrared sea-surface temperature retrievals: Dry air layer intrusions over the tropical ocean," *Remote Sens. Environ.*, vol. 140, pp. 450–465, Jan. 2014.
- [22] F. Xu and A. Ignatov, "In situ SST Quality Monitor (iQuam)," *J. Atmos. Ocean. Technol.*, vol. 31, no. 1, pp. 164–180, Aug. 2013.
- [23] C. J. Donlon *et al.*, "The Operational Sea Surface Temperature and Sea Ice Analysis (OSTIA) system," *Remote Sens. Environ.*, vol. 116, pp. 140–158, Jan. 2012.
- [24] C. L. Gentemann, "Three way validation of MODIS and AMSR-E sea surface temperatures," *J. Geophys. Res., Oceans*, vol. 119, no. 4, pp. 2583–2598, Apr. 2014.
- [25] J. J. Kennedy, "A review of uncertainty in *in situ* measurements and data sets of sea surface temperature," *Rev. Geophys.*, vol. 52, no. 1, pp. 1–32, Mar. 2014.
- [26] R. W. Reynolds, N. A. Rayner, T. M. Smith, D. C. Stokes, and W. Wang, "An improved *in situ* and satellite SST analysis for climate," *J. Clim.*, vol. 15, no. 13, pp. 1609–1625, Jul. 2002.
- [27] S. Eastwood, P. Le Borgne, S. Pétré, and D. Poultier, "Diurnal variability in sea surface temperature in the Arctic," *Remote Sens. Environ.*, vol. 115, no. 10, pp. 2594–2602, Oct. 2011.
- [28] S. Ackerman *et al.*, "Discriminating clear-sky from cloud with MODIS algorithm theoretical basis document (MOD35)," presented at the MODIS Cloud Mask Team, Cooperative Inst. Meteorol. Satellite Studies, Madison, WI, USA, 2010.
- [29] C. J. Merchant, P. Le Borgne, A. Marsouin, and H. Roquet, "Optimal estimation of sea surface temperature from split-window observations," *Remote Sens. Environ.*, vol. 112, no. 5, pp. 2469–2484, May 2008.
- [30] P. Dash, A. Ignatov, Y. Kihai, and J. Sapper, "The SST Quality Monitor (SQUAM)," *J. Atmos. Ocean. Technol.*, vol. 27, no. 11, pp. 1899–1917, Jul. 2010.
- [31] P. Dash *et al.*, "Group for High Resolution Sea Surface Temperature (GHRSST) analysis fields inter-comparisons—Part 2: Near real time web-based Level 4 SST Quality Monitor (L4-SQUAM)," *Deep Sea Res. II, Top. Stud. Oceanogr.*, vol. 77–80, pp. 31–43, Nov. 2012.
- [32] C. J. Merchant and A. R. Harris, "Toward the elimination of bias in satellite retrievals of sea surface temperature: 2. Comparison with *in situ* measurements," *J. Geophys. Res., Oceans*, vol. 104, no. C10, pp. 23 579–23 590, Oct. 1999.
- [33] C. J. Merchant *et al.*, "Deriving a sea surface temperature record suitable for climate change research from the along-track scanning radiometers," *Adv. Space Res.*, vol. 41, no. 1, pp. 1–11, 2008.
- [34] C. J. Merchant *et al.*, "A 20 year independent record of sea surface temperature for climate from along-track scanning radiometers," *J. Geophys. Res., Oceans*, vol. 117, no. C12, Dec. 2012, Art. ID C12013.
- [35] C. J. Donlon *et al.*, "Toward improved validation of satellite sea surface skin temperature measurements for climate research," *J. Clim.*, vol. 15, no. 4, pp. 353–369, Feb. 2002.
- [36] A. G. O'Carroll, J. R. Eyre, and R. W. Saunders, "Three-way error analysis between ATSR, AMSR-E, and *in situ* sea surface temperature observations," *J. Atmos. Ocean. Technol.*, vol. 25, no. 7, pp. 1197–1207, Jul. 2008.
- [37] A. Stoffelen, "Toward the true near-surface wind speed: Error modeling and calibration using triple collocation," *J. Geophys. Res., Oceans*, vol. 103, no. C4, pp. 7755–7766, Apr. 1998.
- [38] F. Xu and A. Ignatov, "Evaluation of *in situ* sea surface temperatures for use in the calibration and validation of satellite retrievals," *J. Geophys. Res., Oceans*, vol. 115, no. C9, Sep. 2010, Art. ID C09022.
- [39] A. G. O'Carroll, T. August, P. Le Borgne, and A. Marsouin, "The accuracy of SST retrievals from Metop-A IASI and AVHRR using the EU-METSAT OSI-SAF matchup dataset," *Remote Sens. Environ.*, vol. 126, pp. 184–194, Nov. 2012.
- [40] K. Lean and R. W. Saunders, "Validation of the ATSR Reprocessing for Climate (ARC) dataset using data from drifting buoys and a three-way error analysis," *J. Clim.*, vol. 26, no. 13, pp. 4758–4772, Jan. 2013.